

Contribution from the Department of Chemistry and Biochemistry, University of Notre Dame, Notre Dame, Indiana 46556, and Department of Chemistry, Princeton University, Princeton, New Jersey 08544

## Influence of Porphyrin Radical Type on V=O Bond Strength in Vanadyl Porphyrin Cation Radicals: Implications for Heme Protein Intermediates

Kathleen A. Macor,<sup>\*,†</sup> Roman S. Czernuszewicz,<sup>‡,§</sup> and Thomas G. Spiro<sup>†</sup>

Received August 18, 1989

Resonance Raman spectra have been analyzed for vanadyl porphyrin cation radicals of octaethylporphyrin (OEP), *meso*-tetraphenylporphyrin (TPP), and *meso*-tetramesitylporphyrin (TMP). The strength of the metal–oxo bond in these cation radicals is demonstrated to be a function of radical type, “ $a_{1u}$ ” or “ $a_{2u}$ ”. Porphyrin ring mode  $\nu_2$ , which has previously been shown to be a marker for the radical type, was used to identify the radicals. The  $a_{1u}$  OV(OEP) radical exhibited an upshift in the V=O stretching frequency resulting from the increased positive charge on the porphyrin, which reduces the porphyrin  $\rightarrow$  vanadium electron donation and increases the O  $\rightarrow$  vanadium donation.  $\nu(\text{V=O})$  frequency decreases were observed for the  $a_{2u}$  OV(TPP) and OV(TMP) radicals. These can be explained on the basis of mixing of the porphyrin  $\pi$   $a_{2u}$  orbital with the vanadium  $d_{z^2}$  and oxygen  $p_z$  orbitals, which is allowed in  $C_{4v}$  symmetry. This interaction decreases the bond strength in  $a_{2u}$  cation radicals, since an electron is removed from an orbital with partial V–O  $\sigma$ -bonding character. Mixing of the porphyrin  $a_{1u}$   $\pi$  orbital with metal or oxygen orbitals is forbidden. These results imply that porphyrin radical type is an important determinant of the Fe=O bond strength in heme protein cation-radical intermediates.

### Introduction

Porphyrins that contain metal–oxo bonds have been extensively studied as models for the heme protein active sites of the peroxidases, catalases, and cytochrome  $P_{450}$ 's. Catalases decompose hydrogen peroxide to oxygen and water, whereas peroxidases oxidize organic and inorganic substrates via reaction with peroxides and other oxidants. The active sites of both enzymes, known as compound I, are porphyrin cation radicals that contain ferryl (Fe=O) bonds. Cytochrome  $P_{450}$ , which hydroxylates a variety of organic molecules via an oxygen atom transfer mechanism, reduces molecular oxygen to generate a ferryl intermediate of the same formal oxidation state as compound I. The catalytic cycles of these enzymes have been extensively reviewed.<sup>1</sup>

There is considerable interest in utilizing metal–oxo porphyrins as catalysts for oxidative reactions, ranging from hydrocarbon oxidation to water splitting.<sup>2</sup> Manganese, chromium, and iron porphyrins react with oxygen atom transfer reagents, such as iodosylbenzene, *m*-chloroperoxybenzoic acid, and sodium hypochlorite, yielding  $\text{Mn}^{\text{VO}}\text{O}^3$  and  $\text{Cr}^{\text{VO}}\text{O}^4$  porphyrins and  $\text{Fe}^{\text{IVO}}$  porphyrin cation radicals.<sup>5</sup> These are potent oxidizing agents that are capable of catalytic oxygen atom insertion into hydrocarbons.  $\text{Fe}^{\text{IVO}}$  porphyrins have been generated via low-temperature decomposition of peroxy-bridged intermediates<sup>6</sup> and irradiation of  $\text{PF}_6\text{FeO}_2$  adducts at 12 K in argon matrices.<sup>7</sup> Electrochemical oxidation in hydroxide-containing solutions has produced both  $\text{Fe}^{\text{IVO}}$ <sup>8</sup> and  $\text{Mn}^{\text{IVO}}$ <sup>3b,9</sup> porphyrins. Resonance Raman spectroscopy has been extensively used to characterize the metal–oxo bonds in ferryl porphyrins<sup>7,8a,10</sup> and proteins,<sup>11</sup> and the  $\text{Mn}^{\text{IV}}=\text{O}$  Raman stretch was recently observed.<sup>9</sup>

Vanadyl porphyrins contain a stable V–O bond and provide a convenient model system for the more reactive ferryl porphyrins. H-bonding and axial ligand interactions have been monitored for V=O porphyrins with resonance Raman spectroscopy.<sup>12</sup> The vanadyl porphyrin cation radical has also been studied,<sup>12</sup> and the V–O stretching frequency was reported to increase 15  $\text{cm}^{-1}$  in OV(OEP)<sup>++</sup> (OEP = octaethylporphyrin).

In the present study we have observed that the direction of the cation-radical shift of the metal–oxo bond frequency is dependent on the spin density pattern of the cation radical. Porphyrin ring mode  $\nu_2$ , which has previously been shown to be marker for radical type,<sup>13</sup> was used to identify the radicals. An upshift of this mode indicates an  $a_{1u}$  radical, while a downshift is characteristic of an  $a_{2u}$  radical. The shift directions have been explained on the basis

of electron removal from antibonding and bonding orbitals, respectively. The  $a_{1u}$  OV(OEP) radical exhibits an upshift in the

- (1) (a) Ortiz de Montellano, P. R. *Acc. Chem. Res.* **1987**, *20*, 289–294. (b) Ortiz de Montellano, P. R., Ed. *Cytochrome P450 Structure, Mechanism, and Biochemistry*; Plenum: New York, 1986. (c) Guengerich, F. P.; MacDonald, T. L. *Acc. Chem. Res.* **1984**, *17*, 9–16. (d) Hewson, W. D.; Hager, L. P. In *The Porphyrins*; Dolphin, D., Ed.; Academic Press: New York, 1979; Vol. 7, Chapter 6. (e) Dunford, H. B.; Stillman, J. S. *Coord. Chem. Rev.* **1976**, *19*, 187–251.
- (2) (a) Creager, S. E.; Raybuck, S. A.; Murray, R. W. *J. Am. Chem. Soc.* **1986**, *108*, 4225–4227. (b) Collman, J. P.; Brauman, J. I.; Meunier, B.; Hayashi, T.; Kodadek, T.; Raybuck, S. A. *J. Am. Chem. Soc.* **1985**, *107*, 2000–2005. (c) Powell, M. F.; Pai, E.; Bruce, T. C. *J. Am. Chem. Soc.* **1984**, *106*, 3277–3285. (d) Harriman, A.; Porter, G.; Walters, P. *J. Chem. Soc., Faraday Trans. 1* **1983**, *79*, 1335–1350.
- (3) (a) Schappacher, M.; Weiss, R. *Inorg. Chem.* **1987**, *26*, 1190–1192. (b) Groves, J. T.; Stern, M. K. *J. Am. Chem. Soc.* **1987**, *109*, 3812–3814. (c) Bortoloni, O.; Meunier, B.; Friant, P.; Ascone, I.; Goulon, J. *Nouv. J. Chim.* **1986**, *10*, 39–49.
- (4) (a) Penner-Hahn, J. E.; Benfatto, M.; Hedman, B.; Takahashi, T.; Sebastian, D.; Groves, J. T.; Hodgson, K. O. *Inorg. Chem.* **1986**, *25*, 2255–2259. (b) Groves, J. T.; Kruper, W. J. *J. Am. Chem. Soc.* **1979**, *101*, 7613–7615.
- (5) (a) Balch, A. L.; La Mar, G. N.; Latos-Grazynsky, L.; Renner, M. W.; Thanabal, V. *J. Am. Chem. Soc.* **1985**, *107*, 3003–3007. (b) Groves, J. T.; Haushalter, R. C.; Nakamura, M.; Nemo, T. E.; Evans, B. J. *J. Am. Chem. Soc.* **1981**, *103*, 2884–2886.
- (6) Chin, D. H.; La Mar, G. N.; Balch, A. L. *J. Am. Chem. Soc.* **1980**, *102*, 5945–5946.
- (7) (a) Proniewicz, L. M.; Bajdor, K.; Nakamoto, K. *J. Phys. Chem.* **1986**, *90*, 1760–1766. (b) Bajdor, K.; Nakamoto, K. *J. Am. Chem. Soc.* **1984**, *106*, 3045–3046.
- (8) (a) Czernuszewicz, R. S.; Macor, K. A. *J. Raman Spectrosc.* **1988**, *19*, 553–557. (b) Groves, J. T.; Gilbert, J. A. *Inorg. Chem.* **1986**, *25*, 123–125. (c) Lee, W.; Calderwood, T. S.; Bruce, T. C. *Proc. Natl. Acad. Sci. U.S.A.* **1985**, *82*, 4301–4305. (d) Calderwood, T. S.; Lee, W. A.; Bruce, T. C. *J. Am. Chem. Soc.* **1985**, *107*, 8272–8273.
- (9) Czernuszewicz, R. S.; Su, Y. O.; Stern, M. K.; Macor, K. A.; Kim, D.; Groves, J. T.; Spiro, T. G. *J. Am. Chem. Soc.* **1988**, *110*, 4158–4165.
- (10) (a) Kincaid, J. R.; Schneider, A. J.; Paeng, K. J. *J. Am. Chem. Soc.* **1989**, *111*, 735–737. (b) Paeng, K. J.; Shiwaku, H.; Nakamoto, K. *J. Am. Chem. Soc.* **1988**, *110*, 1995–1996. (c) Hashimoto, S.; Tatsuno, Y.; Kitagawa, T. *J. Am. Chem. Soc.* **1987**, *109*, 8096–8097. (d) Kean, R. T.; Oertling, W. A.; Babcock, G. T. *J. Am. Chem. Soc.* **1987**, *109*, 2185–2187. (e) Schappacher, M.; Chottard, G.; Weiss, R. *J. Chem. Soc. Chem. Commun.* **1986**, 93–94. (f) Hashimoto, S.; Tatsuno, Y.; Kitagawa, T. In *Proceedings of the Tenth International Conference on Raman Spectroscopy*; University of Oregon Press: Eugene, OR, 1986; p 1-28.
- (11) (a) Paeng, K. J.; Kincaid, J. R. *J. Am. Chem. Soc.* **1988**, *110*, 7913–7915. (b) Ogura, T.; Kitagawa, T. *J. Am. Chem. Soc.* **1987**, *109*, 2177–2179. (c) Hashimoto, S.; Tatsuno, Y.; Kitagawa, T. *Proc. Natl. Acad. U.S.A.* **1986**, *83*, 2417–2421. (d) Turner, J.; Sitter, A. J.; Reczek, C. M. *Biochim. Biophys. Acta* **1985**, *828*, 73–80. (e) Oertling, W. A.; Babcock, G. T. *J. Am. Chem. Soc.* **1985**, *107*, 6406–6407. (f) Van Wart, H. E.; Zimmer, J. *J. Am. Chem. Soc.* **1985**, *107*, 3379–3381.
- (12) Su, Y. O.; Czernuszewicz, R. S.; Miller, L. A.; Spiro, T. G. *J. Am. Chem. Soc.* **1988**, *110*, 4150–4157.
- (13) Czernuszewicz, R. S.; Macor, K. A.; Li, X. Y.; Kincaid, J. R.; Spiro, T. G. *J. Am. Chem. Soc.* **1989**, *111*, 3860–3869.

\* To whom correspondence should be addressed.

<sup>†</sup> University of Notre Dame.

<sup>‡</sup> Princeton University.

<sup>§</sup> Present address: Department of Chemistry, University of Houston, Houston, TX 77004.

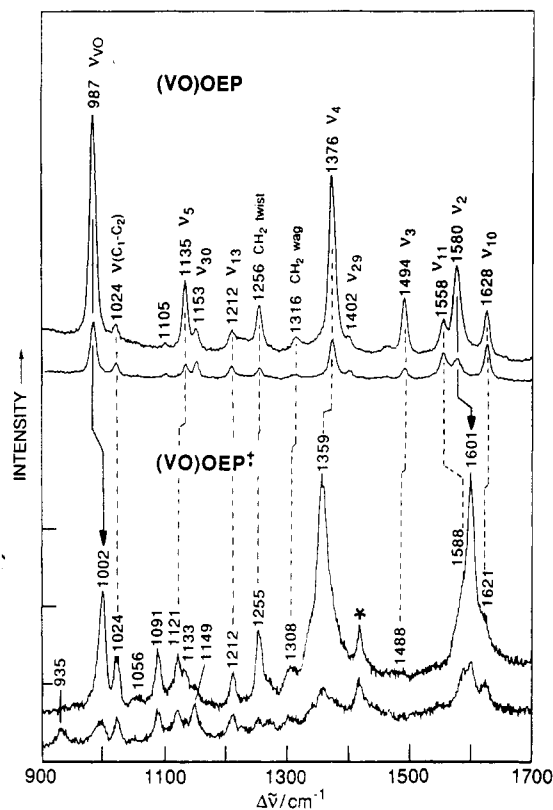


**Figure 1.** Resonance Raman spectra of OV(OEP) and OV(OEP)<sup>•+</sup> in parallel (||) and perpendicular (⊥) polarizations obtained with 406.7-nm excitation. Conditions: 50-mW laser power and 8-cm<sup>-1</sup> slit widths. Asterisks indicate CH<sub>2</sub>Cl<sub>2</sub> solvent bands, and arrows indicate the upshifts of  $\nu(\text{V}=\text{O})$  and  $\nu_2$  modes upon cation-radical formation.

$\text{V}=\text{O}$  stretching frequency from the increased positive charge on the porphyrin, which reduces the porphyrin  $\rightarrow$  vanadium electron donation and increases the  $\text{O} \rightarrow$  vanadium donation.  $\nu(\text{V}=\text{O})$  frequency decreases were observed for the  $a_{2u}$  OV(TPP) (TPP = tetraphenylporphyrin) and OV(TMP) (TMP = tetramesitylporphyrin) radicals. These can be explained on the basis of mixing of the porphyrin  $\pi a_{2u}$  with the vanadium  $d_{z^2}$  and oxygen  $p_z$  orbitals, which is allowed in  $C_{4v}$  symmetry. This interaction decreases the bond strength in  $a_{2u}$  cation radicals, since an electron is removed from an orbital with partial  $\text{V}-\text{O}$   $\sigma$ -bonding character. Mixing of the porphyrin  $a_{1u}$   $\pi$  orbital with metal or oxygen orbitals is forbidden.

These results imply that porphyrin radical type is an important determinant of the  $\text{Fe}=\text{O}$  bond strength in heme protein cation-radical intermediates.

### Experimental Section

**Chemicals.** Vanadyl octaethyl-, *meso*-tetraphenyl-, and *meso*-tetramesitylporphyrins were obtained from Mid-Century Chemicals (Posen, IL) and were purified on thin-layer alumina plates. Tetrabutylammonium perchlorate (TBAP) (GFS Chemicals, Columbus, OH) was recrystallized from ethyl acetate and dried under vacuum at 90 °C. CH<sub>2</sub>Cl<sub>2</sub> was distilled over CaH<sub>2</sub> prior to use. The <sup>18</sup>O-vanadyl isomers were prepared from the dichlorovanadium(IV) porphyrins, which were supplied by Mid-Century Chemicals, by treatment with H<sub>2</sub><sup>18</sup>O (Cambridge Isotopes, Boston, MA).

**Oxidations.** Vanadyl porphyrin cation radicals were prepared by controlled-potential electrolysis of the oxovanadium(IV) porphyrins in 0.1 M TBAP/CH<sub>2</sub>Cl<sub>2</sub> with a Princeton Applied Research 173 potentiostat, 175 programmer, and 179 coulometer. The three-electrode Raman spectroelectrochemical cell was described previously.<sup>8a</sup> A Pt anode and saturated calomel reference electrode were used. The oxidations were carried at room temperature and -80 °C for OV(OEP) and OV(TPP), respectively. A small amount of irreversible porphyrin decomposition was observed when OV(TPP) was oxidized at room temperature; at low temperature oxidation was reversible, however. The course of electrooxidation was followed by monitoring porphyrin Raman band  $\nu_2$ , since the position of this band is sensitive to porphyrin ring oxidation. Following oxidation and cation radical data acquisition, the solutions

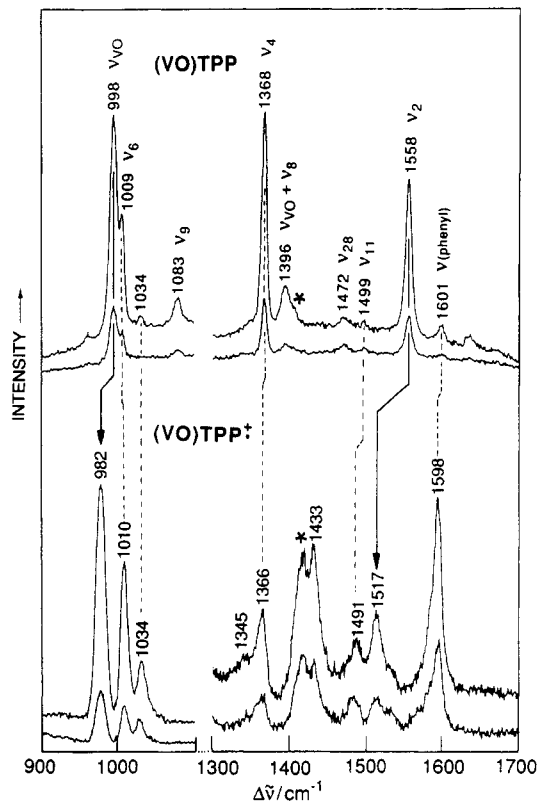


**Figure 2.** Resonance Raman spectra of OV(TPP) and OV(TPP)<sup>•+</sup> in parallel (||) and perpendicular (⊥) polarizations obtained with 406.7- (900–1100 cm<sup>-1</sup>) and 457.9-nm (1300–1700 cm<sup>-1</sup>) excitation. Conditions are as in Figure 1. Asterisks indicate CH<sub>2</sub>Cl<sub>2</sub> solvent bands, and arrows indicate the downshifts of  $\nu(\text{V}=\text{O})$  and  $\nu_2$  modes upon cation-radical formation.

were reduced at 0.2 V. In each case the neutral species spectrum was recovered.

**Raman Measurements.** Resonance Raman spectra were obtained in backscattering geometry from porphyrin solutions by using the Raman spectroelectrochemical cell<sup>8a</sup> previously described. Exciting radiation was provided by Coherent Radiation Innova 100K-3 krypton and Spectra Physics Model 2025 argon ion lasers. The scattered radiation was dispersed by a Spex 1401 double monochromator and detected by a cooled RCA 31034A photomultiplier tube using an Ortec 9315 photon-counting system, under the control of an IBM XT computer.

### Results

The high frequency region resonance Raman (RR) spectra shown in Figures 1 and 2 identify the OV(OEP) and OV(TPP) radicals as  $a_{1u}$  and  $a_{2u}$ , respectively, on the basis of the shift directions of porphyrin ring mode  $\nu_2$  upon cation-radical formation. It has previously been shown from a study of metalated OEP and TPP radicals<sup>13</sup> that mode  $\nu_2$  is an indicator of radical type, shifting down 25–40 cm<sup>-1</sup> for  $a_{2u}$  radicals and displaying 20–25 cm<sup>-1</sup> upshifts for  $a_{1u}$  radicals.  $\nu_2$  is composed of mainly pyrrole  $\text{C}_\beta\text{C}_\beta$  stretching. The  $\text{C}_\beta\text{C}_\beta$  interaction is bonding and antibonding, in the  $a_{2u}$  and  $a_{1u}$  orbitals, respectively (see Figure 4a). Removing an electron from the former orbital results in a weaker bond with a lower stretching frequency, whereas a higher stretching frequency is observed for the latter, since the electron is removed from an antibonding orbital. Band  $\nu_2$  is seen at 1580 cm<sup>-1</sup> in OV(OEP). It shifts up 21 cm<sup>-1</sup> to 1601 cm<sup>-1</sup> in OV(OEP)<sup>•+</sup> (Figure 1), whereas a 41-cm<sup>-1</sup> downshift is observed from 1558 cm<sup>-1</sup> in OV(TPP) to 1517 cm<sup>-1</sup> in OV(TPP)<sup>•+</sup> (Figure 2). A downshift of 40 cm<sup>-1</sup> was also seen for OV(TMP)<sup>•+</sup>, whose spectrum (not shown) is similar to that of OV(TPP)<sup>•+</sup>.

The strong band at 1598 cm<sup>-1</sup> in the spectrum of OV(TPP)<sup>•+</sup> (Figure 2) is phenyl mode  $\nu_{8a}$ , which appears at 1601 cm<sup>-1</sup> in OV(TPP). Phenyl mode intensity increases are characteristic of porphyrin cation radicals<sup>13</sup> and may result from a tilt of the phenyl rings toward planarity with the porphyrin ring, which has been observed in cation radical X-ray crystal structures.<sup>14</sup>

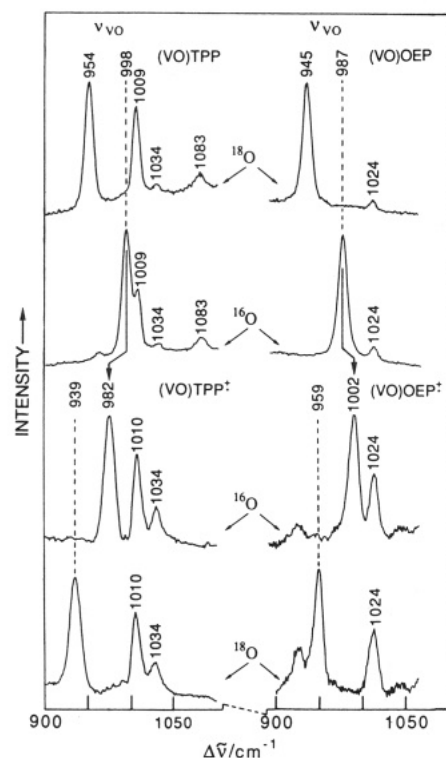


**Figure 3.** Resonance Raman spectra of OV(TPP) and OV(TPP)<sup>•+</sup> (left panel) and OV(OEP) and OV(OEP)<sup>•+</sup> (right panel) and their <sup>18</sup>O-isotopomers obtained with 406.7-nm excitation. Conditions are as in Figure 1. The arrows indicate shifts of  $\nu(\text{V}=\text{}^{16}\text{O})$  upon cation-radical formation.

The metal-oxo bond strength decreases upon formation of the  $a_{2u}$  OV(TPP) radical, whereas the opposite effect occurs in the  $a_{1u}$  OV(OEP) radical. The  $\text{V}=\text{O}$  stretch seen at  $987\text{ cm}^{-1}$  in the OV(OEP) spectrum in Figure 1 shifts up  $15\text{ cm}^{-1}$  to  $1002\text{ cm}^{-1}$  in the radical. In contrast, this band observed at  $998\text{ cm}^{-1}$  in OV(TPP) exhibits a  $16\text{-cm}^{-1}$  downshift to  $982\text{ cm}^{-1}$  in OV(TPP)<sup>•+</sup> (Figure 2). A downshift of  $14\text{ cm}^{-1}$  was also observed for OV(TMP)<sup>•+</sup>. The  $\text{V}=\text{O}$  stretching bands were identified by the  $43\text{-cm}^{-1}$  downshifts observed for the unoxidized and cation-radical porphyrins containing <sup>18</sup>O-labels.  $\nu(\text{V}=\text{}^{18}\text{O})$  is observed at  $959$  and  $939\text{ cm}^{-1}$  in the <sup>18</sup>O adducts of OV(OEP)<sup>•+</sup> and OV(TPP)<sup>•+</sup>, respectively, as seen in Figure 3.

The  $\text{V}=\text{O}$  stretching mode is one of the strongest bands in the Soret-excited resonance Raman spectra. The Soret transition populates the set of lowest unoccupied porphyrin orbitals ( $e_g^*$ ), which are mixed with the antibonding  $d_{xz}-\text{O } p_x$  and  $d_{yz}-\text{O } p_y$  orbitals ( $e_g^*$ ) (see Figure 5). Metal-ligand modes are enhanced to the extent that the metal-ligand bond lengths are altered in the resonant excited state.<sup>15</sup> Population of the  $e_g^*$  orbital in the excited state lengthens the  $\text{V}-\text{O}$  bond due to competition with the oxygen  $\pi$  electrons for the empty  $d_\pi$  vanadium orbitals. The relative intensities indicate that the  $\text{V}-\text{O}$  bond lengthening is comparable to the alteration of the porphyrin ring bonds in the excited state.

## Discussion

**1. Mechanisms for  $\nu(\text{V}=\text{O})$  Frequency Change in Cation Radicals. A. Polarization Effect.** The metal-oxo bond strength increases upon formation of the  $a_{1u}$  OV(OEP) radical. The  $\text{V}=\text{O}$  stretch seen at  $987\text{ cm}^{-1}$  in the OV(OEP) spectrum in Figure 1 shifts up  $15\text{ cm}^{-1}$  to  $1002\text{ cm}^{-1}$  in the radical. An increase in frequency is expected on the basis of bond polarization; the one-electron deficient porphyrin radical cation donates less electron density to vanadium, resulting in increased  $\text{O} \rightarrow \text{V}$  donation and

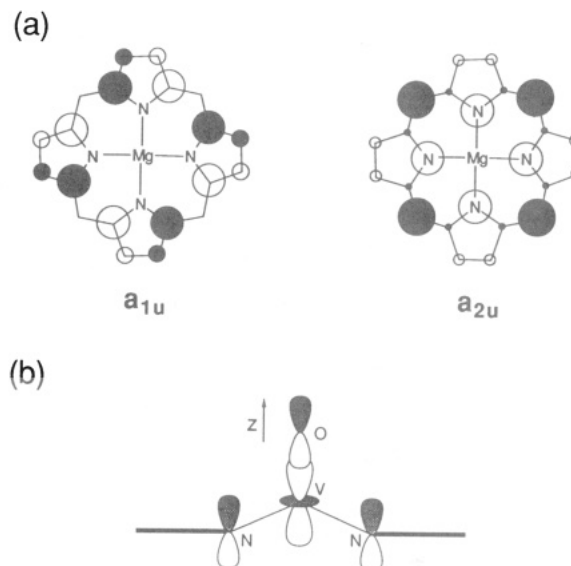


**Figure 4.** (a) Atomic orbital (AO) structure of magnesium porphyrin in the two highest occupied molecular orbitals,  $a_{1u}$  and  $a_{2u}$ . The circle sizes are approximately proportional to the AO coefficients.<sup>13</sup> The open circles represent negative signs of the upper lobe of the  $p_x$  AO's. (b) Illustration of the porphyrin  $a_{2u}$ , vanadium  $d_{2z}$ , and oxygen  $p_z$   $\sigma$ -bonding interaction, which is responsible for the  $\nu(\text{V}=\text{O})$  downshift in  $a_{2u}$  porphyrin cation radicals. (Only two porphyrin nitrogens are shown.) The shaded circles represent negative signs of the orbitals.

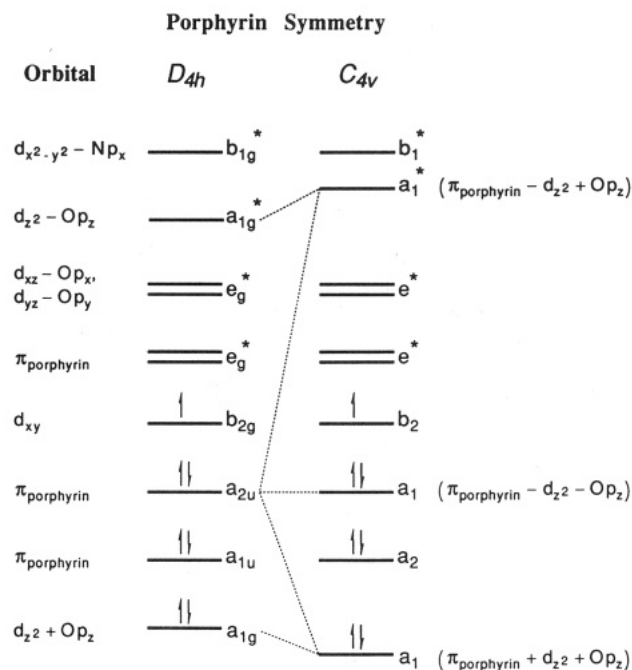


**Figure 5.** Qualitative  $D_{4h}$  and  $C_{4v}$  orbital energy level diagram, which illustrates the mixing between the porphyrin  $a_{2u}$ , metal  $d_{z^2}$ , and oxygen  $p_z$  orbitals in  $C_{4v}$  symmetry. Mixing of the porphyrin  $a_{1u}$  orbital with metal or oxygen orbitals is forbidden. In  $D_{4h}$  symmetry, no interactions are possible between the  $a_{2u}$  or  $a_{1u}$  HOMO's and any metal orbitals (all of which are "g").

a stronger  $\text{V}=\text{O}$  bond. The magnitude of the shift is comparable to the difference in  $\nu(\text{V}=\text{O})$  between OV(TMPyP) (TMPyP = tetrakis(methylpyridiniumyl)porphyrin) and OV(TPP),  $17\text{ cm}^{-1}$  (in nonacceptor solvents).<sup>12</sup> OV(TMPyP) has four positive charges on the four peripheral pyridyl groups. It seems reasonable that their inductive effect is about the same as that of a single positive charge on the porphyrin ring itself. The inductive effect should be even larger for an  $a_{2u}$  than an  $a_{1u}$  radical, since the former concentrates charge on the pyrrole N atoms, which are bonded to the vanadium, whereas the  $a_{1u}$  orbital has nodes at the N atoms. Consequently, the downshift associated with radical formation

(14) Scheidt, W. R.; Lee, Y. J. *Struct. Bonding* **1987**, *64*, 1-70 and references therein.

(15) Spiro, T. G. In *Iron Porphyrins*; Lever, A. B. P., Gray, H. B., Eds.; Addison-Wesley: Reading, MA, 1983; Part II, pp 89-159.

in OV(TPP) and OV(TMP) requires an additional mechanism.

**B. Steric Factors.** The possibility needs to be considered that the altered peripheral substituents are themselves responsible for bonding differences between OV(OEP)<sup>•+</sup> and OV(TPP)<sup>•+</sup> and OV(TMP)<sup>•+</sup>. We note that TPP cation radicals frequently display saddle-shaped structures<sup>14</sup> in which the phenyl rings are rotated significantly toward the porphyrin plane and the pyrrole rings are displaced alternately up and down. This concerted distortion might be an intrinsic electronic effect, since the  $a_{2u}$  radicals concentrate charge on the methine bridges (as well as the porphyrin N atoms) and this charge could be delocalized onto the phenyl  $\pi$  systems to the extent that the phenyl and porphyrin  $\pi$  orbitals approach coplanarity. If the saddle distortion is intrinsic and is specific to TPP, it might explain the V=O frequency decrease because there would be increased nonbonded repulsion between two pyrrole N atoms (the two upwardly displaced pyrroles) and the vanadyl O atom.

However, Scheidt<sup>14</sup> has argued that the tilt of the phenyl rings is an intermolecular effect, since it allows a close approach of two porphyrin rings. All the saddle-distorted TPP radical structures do show dimer formation in the solid. Supporting this view is the recent finding that Cu(TMP)<sup>•+</sup> is monomeric in the solid state,<sup>16</sup> the bulky mesityl groups presumably inhibiting dimer formation, and the porphyrin ring is planar. Since we find the same  $\nu(\text{V=O})$  downshift for OV(TMP)<sup>•+</sup> as for OV(TPP)<sup>•+</sup>, it seems very unlikely that the effect can be attributed to steric factors.

**C. HOMO Differences.** We offer an explanation for the V=O bond weakening in  $a_{2u}$  radicals based on orbital mixing, which becomes permitted upon symmetry reduction from  $D_{4h}$  to  $C_{4v}$ . Figure 5 provides a qualitative  $D_{4h}$  and  $C_{4v}$  orbital energy level diagram. The highest occupied orbital (HOMO) of a  $D_{4h}$  metalloporphyrin is  $a_{1u}$  or  $a_{2u}$  depending upon a combination of factors including porphyrin ring substituents and axial ligands.<sup>17</sup> The  $\text{O}^{2-}$  ligand donates  $\sigma$  and  $\pi$  electrons to the  $\text{V}^{4+}$  ion. The filled  $p_x$  orbitals on the ligand ( $p_x$  and  $p_y$ , with  $z$  as the M–O direction) interact with the  $d_x$  orbitals ( $d_{xz}$ ,  $d_{yz}$ ), which become antibonding. The  $d_{z^2}$  and  $d_{x^2-y^2}$  orbitals are  $\sigma$  antibonding with respect to the V–O bond and the V–N bonds, respectively, and are at higher energy. The  $d_{xy}$  orbital is nonbonding. This orbital accommodates the single d electron of  $\text{V}^{4+}$ , allowing unimpeded  $\text{O} \rightarrow \text{M}$   $\pi$  interactions. Since there are two  $\pi$  orbital overlaps, the result is formally a  $\text{M=O}$  triple bond. EPR spectroscopy<sup>18</sup> indicates that there is one unpaired electron on the vanadium in a relatively pure  $d_{xy}$  orbital in the unoxidized porphyrin and that one-electron oxidation removes an electron from a porphyrin orbital.

In  $D_{4h}$  symmetry, no interactions are possible between the porphyrin  $a_{2u}$  or  $a_{1u}$  HOMO's and any metal orbitals (all of which are "g"). When the symmetry is  $C_{4v}$ , however, the  $a_{2u}$  and  $d_{z^2}$  orbitals both become  $a_1$ . Orbital overlap becomes possible because the V atom is displaced (by 0.5 Å<sup>19</sup>) from the porphyrin plane. Because the  $d_{z^2}$  orbital interacts strongly with the oxygen  $p_z$  orbital, three orbitals are produced by the  $a_{2u}$  interaction. The orbital of lowest energy (Figure 5) is completely bonding (zero nodes) and contains two electrons. The highest energy orbital has two nodes and is antibonding with respect to both the porphyrin–vanadium and the vanadium–oxygen interactions. This orbital is unoccupied. The middle energy orbital, which is the HOMO, contains one node and is, to first-order,  $\sigma$  nonbonding with respect to the V–N and V–O bonds. However, orbital mixing imparts a small amount of  $d_{z^2} + \text{O } p_z$  character to the HOMO. Figure 4b illustrates the V–O–porphyrin bonding interaction. Consequently, removing an electron partially weakens the O–V  $\sigma$  bond

and can account for the  $\sim 15\text{-cm}^{-1}$  downshift observed for the " $a_{2u}$ " OV(TPP)<sup>•+</sup> and OV(TMP)<sup>•+</sup> radicals. This mechanism is unavailable to OV(OEP)<sup>•+</sup>, since the  $a_{1u}$  orbital ( $a_2$  in  $C_{4v}$  symmetry) remains unable to mix with the vanadium orbitals.

EPR spectra of halide-ligated Zn and Co(TPP) cation radicals exhibit metal and axial ligand hyperfine splitting.<sup>20</sup> Such splitting is observed along with nitrogen hyperfine splitting, which designates the radicals as  $a_{2u}$ , since electron density is mainly localized on the nitrogens and meso carbons in these radicals. These results clearly indicate that in  $a_{2u}$  radicals spin density is transmitted to axial ligands via the nitrogens. In contrast,  $a_{1u}$  radicals have little, if any, spin density on the nitrogens and are without a mechanism to deliver spin density to axial ligands. Charge-iterative extended Hückel calculations on ferryl porphyrins have also indicated that a small amount of spin density resides on the oxo ligand in  $a_{2u}$ , but not  $a_{1u}$ , radicals.<sup>21</sup>

**2. Implications for Heme Proteins.** Recently, a  $41\text{-cm}^{-1}$  downshift of  $\nu(\text{Fe=O})$  along with a  $\sim 40\text{-cm}^{-1}$  downshift for porphyrin mode  $\nu_2$  was reported for  $\text{OFe(TMP)}^{\bullet+}$ <sup>10a</sup> generated by *m*-chloroperoxybenzoic acid oxidation of  $\text{Fe(TMP)Cl}$  in toluene at  $-80^\circ\text{C}$ . The ferryl TMP adduct was prepared by cleavage of the peroxy-bridged species also in toluene.<sup>10b,f</sup> The  $\nu_2$  shift indicates that  $\text{OFe(TMP)}^{\bullet+}$  is an  $a_{2u}$  radical, as expected, and the downshift of  $\nu(\text{Fe=O})$  is in accord with the orbital-mixing mechanism. The fact that the shift is substantially larger than that seen for OV(TMP)<sup>•+</sup> ( $41$  vs  $14\text{ cm}^{-1}$ ) suggests that the orbital mixing is also greater for  $\text{OFe(TMP)}^{\bullet+}$ . This can be understood on the basis of a better energy match between the  $a_{2u}$  orbital and the  $\text{Fe } d_{z^2} + \text{O } p_z$  orbital, due to the weaker Fe–O bond. Fe(IV) has three more electrons than V(IV), and the  $\text{Fe } d_x - \text{O } p_x$   $e_g^*$  orbitals (Figure 5) each contain one electron. Consequently the M–O bond order is reduced to two,<sup>9</sup> and  $\nu(\text{Fe=O})$ ,  $843\text{ cm}^{-1}$ , is substantially lower than  $\nu(\text{V=O})$ ,  $991\text{ cm}^{-1}$ . The weaker Fe–O bond implies a smaller  $\sigma$  overlap and consequently a higher energy for the  $d_{z^2} + p_z$  orbital than for the V–O bond. This energy increase would lead to more extensive mixing with the  $a_{2u}$  orbital, thereby increasing the  $\nu(\text{M=O})$  shift.

The present work has implications for the vibrational structures of oxidative heme proteins. HRP compound I has been inferred to contain an  $a_{2u}$  radical ferryl heme, on the basis of EPR,<sup>22</sup> Mössbauer,<sup>22a,23</sup> and ENDOR<sup>24</sup> evidence. Although proto-porphyrin, like OEP, is expected to produce  $a_{1u}$  radicals, the  $a_{2u}$  orbital could become the HOMO through the donor effect of the sixth ligand, imidazole, provided by the protein. This inversion would be consistent with the electronic structure calculations<sup>20a,21</sup> of Hanson et al. Mixing of  $a_{1u}$  and  $a_{2u}$  orbitals is expected (and calculated<sup>21</sup>) because the very different axial ligands, imidazole and oxo, impose  $C_{4v}$  symmetry. If the  $a_{2u}$  assignment is correct, then a weakened Fe=O bond would be expected for compound I in relation to compound II, which contains a ferryl neutral porphyrin.<sup>1d</sup> In a recent resonance Raman study of HRP compound I<sup>11a</sup> a  $39\text{-cm}^{-1}$  downshift of  $\nu(\text{Fe=O})$  has, in fact, been reported along with a  $15\text{-cm}^{-1}$  downshift of mode  $\nu_2$ , the expected direction for an  $a_{2u}$  radical. However, another resonance Raman study of compound I<sup>25</sup> reports an upshifted  $\nu_2$  mode. Assignment of this band is complicated by the presence of multiple bands in the  $1550\text{--}1650\text{-cm}^{-1}$  region in both spectra. In addition, different laser excitations ( $356.4$  vs  $406.7\text{ nm}$ ) were used in the two studies

- (16) Song, H.; Reed, C. A.; Scharif, W. R. *J. Am. Chem. Soc.* **1989**, *111*, 6865–6866.
- (17) Fajer, J.; Borg, D. C.; Forman, A.; Dolphin, D.; Felton, R. H. *J. Am. Chem. Soc.* **1970**, *92*, 3451–3459.
- (18) (a) Lin, W. C. In *The Porphyrins*; Dolphin, D., Ed.; Academic Press: New York, 1979; Vol. 4, Chapter 7. (b) Luckhurst, G. R.; Setaka, M.; Subramanian, J. *Mol. Phys.* **1976**, *32*, 1299–1309. (c) Newton, C. M.; Davis, D. G. *J. Magn. Reson.* **1975**, *20*, 446–457.
- (19) (a) Drew, M. G.; Mitchell, P. C.; Scott, C. E. *Inorg. Chim. Acta* **1984**, *82*, 63–67. (b) Molinaro, F. S.; Ibers, J. A. *Inorg. Chem.* **1976**, *15*, 2278–2282.

- (20) (a) Fujita, I.; Hanson, L. K.; Walker, F. A.; Fajer, J. *J. Am. Chem. Soc.* **1983**, *105*, 3296–3300. (b) Fajer, J.; Davis, M. S. In *The Porphyrins*; Dolphin, D., Ed.; Academic Press: New York, 1979; Vol. 4, Chapter 4. (c) Fajer, J.; Borg, D. C.; Forman, A.; Felton, R. H.; Vegh, L.; Dolphin, D. *Ann. N.Y. Acad. Sci.* **1973**, *206*, 349–364.
- (21) Hanson, L. K.; Chang, C. K.; Davis, M. S.; Fajer, J. *J. Am. Chem. Soc.* **1981**, *103*, 663–670.
- (22) (a) Rutter, R.; Valentine, M.; Hendrich, M. P.; Hager, L. P.; Debrunner, P. G. *Biochemistry* **1983**, *22*, 4769–4774. (b) Roberts, J. E.; Hoffman, B. M.; Rutter, R.; Hager, L. P. *J. Am. Chem. Soc.* **1981**, *103*, 7654–7656.
- (23) Schulz, C. E.; Devaney, P. W.; Winkler, H.; Debrunner, P. G.; Doan, N.; Chiang, R.; Rutter, R.; Hager, L. P. *FEBS Lett.* **1979**, *103*, 102–105.
- (24) Roberts, J. E.; Hoffman, B. M.; Rutter, R.; Hager, L. P. *J. Biol. Chem.* **1981**, *256*, 2118–2121.
- (25) Palaniappan, V.; Terner, J. *J. Biol. Chem.*, in press.

so that direct comparison of the spectra is not possible. Band  $\nu_2$  might be more reliably identified by reconstituting HRP with mesoporphyrin in which the peripheral vinyl groups are replaced with ethyl groups and the  $\nu_2$  region is simplified.<sup>26</sup> It has been argued that the similar methyl  $^1\text{H}$  NMR contact shifts for mesohemin- and native-HRP indicate that they have the same ground state and that the small downfield methine bridge proton contact shift observed for mesohemin-HRP is consistent with an  $a_{1u}$  ground-state assignment.<sup>27</sup>

Whatever the situation turns out to be for HRP, the cytochrome  $P_{450}$  compound I-like intermediate<sup>28</sup> is very likely to involve an  $a_{2u}$  radical. This is because the sixth ligand is the thiolate group of a cysteine residue.<sup>29</sup> Thiolate is a strong donor ligand, as is evident from the marked lowering of the Fe–C stretch of cytochrome  $P_{450}$  CO adducts relative to imidazole–heme CO adducts<sup>30</sup>

and also the anomalously low  $\nu_4$  porphyrin frequency in the reduced enzyme.<sup>31</sup> Porphyrin mode  $\nu_4$  is composed of mainly pyrrole ring  $C_\alpha$ –N and  $C_\alpha$ – $C_\beta$  stretching<sup>32</sup> and is sensitive to the central metal oxidation state and the axial ligand electron donation.<sup>33</sup> Thiolate is even more likely than imidazole to push the  $a_{2u}$  orbital above the  $a_{1u}$  (although the electronic structure calculations have not shown the stronger thiolate donor effect<sup>20a,21</sup>). Consequently, the Fe–O bond in the  $P_{450}$  intermediate should be weakened by two effects, the direct influence of the trans-ligand electron donation<sup>12,34</sup> and the porphyrin radical character. Both are expected to play important roles in the oxygen-transfer chemistry of the enzyme.

**Acknowledgment.** This work was supported by Grant DE-AC02-81-ER-10861 from the U.S. Department of Energy (T.G.S.). We thank Professor James Turner (Virginia Commonwealth University) for communicating results prior to publication.

- (26) Verna, A. L.; Mendelsohn, R.; Bernstein, H. J. *J. Chem. Phys.* **1974**, *61*, 383–387.
- (27) LaMar, G. N.; Thanabal, V.; Johnson, R. D.; Smith, K. M.; Parish, D. W. *J. Biol. Chem.* **1989**, *264*, 5428–5434.
- (28) Groves, J. T.; Haushalter, R. C.; Nakamura, M.; Nemo, T. E.; Evans, B. J. *J. Am. Chem. Soc.* **1981**, *103*, 2884–2886.
- (29) (a) Poulos, T. L.; Finzel, B. C.; Howard, A. J. *Biochemistry* **1986**, *25*, 5314–5322. (b) Champion, P. M.; Stallard, B. R.; Wagner, G. C.; Gunsalus, I. C. *J. Am. Chem. Soc.* **1982**, *104*, 5469–5472. (c) Dawson, J. H.; Holm, R. H.; Trudell, J. R.; Barth, G.; Linder, R. E.; Bunnenberg, E.; Djerassi, C. *J. Am. Chem. Soc.* **1976**, *98*, 3707–3709. (d) Stern, J. O.; Peisach, J. *J. Biol. Chem.* **1974**, *249*, 7495–7480.
- (30) (a) Li, X. Y.; Spiro, T. G. *J. Am. Chem. Soc.* **1988**, *110*, 6033–6046. (b) Champion, P. M. In *Biological Applications of Raman Spectroscopy*; Spiro, T. G., Ed.; John Wiley & Sons: New York, 1988; Vol. 3, Chapter 6. (c) Tsubaki, M.; Ichikawa, Y. *Biochemistry* **1986**, *25*, 3563–3570.
- (31) (a) Anzenbacher, P.; Evangelista-Kirkup, R.; Spiro, T. G. *Inorg. Chem.* **1989**, *28*, 4491–4495. (b) Ozaki, Y.; Kitagawa, T.; Kyogoku, Y.; Shimada, H.; Iizuka, T.; Ishimura, Y. *J. Biochem. (Tokyo)* **1976**, *80*, 1447–1451. (c) Champion, P. M.; Remba, R. D.; Chiang, R.; Fitchen, D. B.; Hager, L. P. *Biochem. Biophys. Acta* **1976**, *446*, 486–490.
- (32) (a) Li, X. Y.; Czernuszewicz, R. S.; Kincaid, J. R.; Su, Y. O.; Spiro, T. G. *J. Phys. Chem.* **1990**, *94*, 31–47. (b) Li, X. Y.; Czernuszewicz, R. S.; Kincaid, J. R.; Stein, P.; Spiro, T. G. *J. Phys. Chem.* **1990**, *94*, 47–61.
- (33) Spiro, T. G. In *Biological Applications of Raman Spectroscopy*; Spiro, T. G., Ed.; John Wiley & Sons: New York, 1988; Vol. 3, Chapter 1.
- (34) (a) Gaul, E. M.; Kassner, R. J. *Inorg. Chem.* **1986**, *25*, 3734–3740. (b) Buchler, J. W.; Kokisch, W.; Smith, P. D. In *Structure and Bonding*; Springer-Verlag: Berlin, 1978; Vol. 34, 79–134.